https://doi.org/10.5194/egusphere-2026-6120
Preprint. Discussion started: 24 November 2026
© Author(s) 2026. CC BY 4.0 License.

Homogenisation of the Arosa/Davos total column ozone time series

Fernanda Cabello Hermosilla[1,2,3], Julian Gröbner[1], Luca Egli[1], Franz Zeilinger[1], Eliane Maillard Barras[4], Rolf Ruefenacht[4], and Gunter Stober[2,3]

[1]Physikalisch-Meteorologisches Observatorium Davos and World Radiation Center (PMOD/WRC), Davos, Switzerland.
[2]Institute of Applied Physics, University of Bern, Bern, Switzerland.
[3]Oeschger Centre for Climate Change Research (OCCR), Bern, Switzerland.
[4]Federal Meteorology and Climatology, Payerne, Switzerland.

Correspondence: Fernanda Cabello Hermosilla (fernanda.cabello@pmodwrc.ch)

Abstract. The assessment of ozone recovery critically relies on high-quality and long-term observations. Using the world's longest continuous Total Column Ozone (TCO) time series (1926-present), we produced a homogenised TCO time series based on six collocated spectrophotometers covering the period from 1990 to 2024, focusing on the implementation of the Montreal protocol and the subsequent recovery period. This study proposes a method for producing the TCO Brewer dataset, based on the instrument standard lamp records and the calibrations performed during the Regional Brewer Calibration Campaigns for Europe (RBCC-E). Regarding the TCO Dobson dataset, following an approach similar to that used for the Brewers, the standard lamp methodology has been implemented as part of the operational measurement procedure.

One of the strengths of this dataset is the way in which the uncertainty is derived for the Brewer and the Dobson instruments, based on their most relevant instrumental parameters. This is done in order to generate a composite dataset with lower uncertainty based on six collocated instruments. In order to preserve the homogeneity of the time series, the relocation of the instruments from Arosa to Davos, which took place from 2011 to 2021, was assessed in great detail. The comparison showed that the relative differences in TCO observed between the two sites of $0.33 \pm 0.78\%$, which is in good agreement with the differences in the calculated tropospheric ozone content between the two locations ($0.28 \pm 0.13\%$). The homogenised data set presents a data coverage of $\sim 90\%$ between 1990 and 2024, with missing data mainly due to bad weather conditions precluding any measurements. The agreements and stabilities of the instruments with respect to the composite data set were mostly within 1%.

Remarkably, the seasonal discrepancies between the Brewer and the Dobson were significantly reduced by incorporating ozone absorption cross-sections measured at the University of Bremen, the ozone effective temperature, and the scattering and stray light effect in the instruments.

https://doi.org/10.5194/egusphere-2026-6120
Preprint. Discussion started: 24 November 2026
© Author(s) 2026. CC BY 4.0 License.

1 Introduction

The ozone layer is projected to recover to levels comparable to those observed during the pre-depletion period by the middle of the 21st century, reflecting the long-term effectiveness of the Montreal Protocol adopted in 1987 and its subsequent amendments, which established controls on the production and consumption of chlorofluorocarbons (CFCs) and other ozone-depleting substances (ODSs). The resulting progressive phase-out of these compounds has led to a decline in their atmospheric concentrations, which has limited further ozone depletion and substantially reduced the associated risk of enhanced ultraviolet (UV) radiation reaching the Earth's surface (Egorova et al., 2013). Nevertheless, since the discovery of the ozone hole (Farman et al., 1985), the atmospheric composition has changed, mainly due to increased emissions of CO_2 and other greenhouse gases, with implications for rising global lower tropospheric temperatures. Understanding the impact of climate change on ozone layer recovery remains a challenge (Chipperfield and Bekki, 2024).

Recent studies have highlighted a strong coupling between stratospheric ozone and climate change (Chipperfield et al., 2017). Climate change is expected to enhance the Brewer–Dobson circulation, which transports ozone from the primary tropical production region to the extratropics; furthermore, chemistry interactions will change as a result of increasing stratospheric concentrations of gases such as CH_4 and N_2O (Butchart, 2014; Chipperfield and Bekki, 2024). In addition, increasing CO_2 concentrations are expected to cool the upper stratosphere, which can reduce the rates of the gas-phase ozone destruction reactions and contribute to enhanced ozone recovery in this region (Hegglin et al., 2015; Chipperfield et al., 2017, and references therein). This so-called "super-recovery" scenario illustrates how changes in atmospheric composition and climate may influence the magnitude and rate of future ozone recovery. Nevertheless, ozone recovery has been a slow process and the detectability and statistical significance of a long-term ozone trend depend on its magnitude relative to the underlying atmospheric variability and observational noise (Steinbrecht et al., 2018). Consequently, an accurate estimation of long-term trends requires a combination of high-quality measurements from multiple instruments (Hassler et al., 2014).

Maintaining long-term observations is difficult due to changes in the instrument, relocations, modifications to calibration procedures, and inter-instrument inconsistencies, all of which create inhomogeneities in the time series. Dobson and Brewer spectrophotometers are the most widely used ground-based instruments for measuring Total Column Ozone (TCO) and ozone profiles, through Direct Sun (DS) (Kerr et al., 1980) and Umkehr measurements (Götz et al., 1934; Petropavlovskikh et al., 2005) respectively. Seasonal differences between these instruments, driven mainly by the temperature-dependent ozone absorption cross-section and the seasonal variability of ozone effective temperature, have been observed over the past decade (Staehelin et al., 1998a; Scarnato et al., 2010; Redondas et al., 2014; Gröbner et al., 2021; Voglmeier et al., 2024) and amendments to the retrieval algorithms proposed for reconciling the datasets (Gröbner et al., 2021; Voglmeier et al., 2024).

TCO satellite measurements now span more than three decades, and the TCO datasets produced from these observations have utilized ground-based observations from Dobson and Brewer spectrophotometers — available from the World Ozone and Ultraviolet Radiation Data Centre (WOUDC) — for validation purposes or as part of merged satellite–ground products (Labow et al., 2013; Bodeker et al., 2021). Additionally, these ground-based measurements have been used to remove systematic biases and drifts from merged satellite products (Bodeker et al., 2021). Therefore, developing a homogenised ground-based reference

https://doi.org/10.5194/egusphere-2026-6120
Preprint. Discussion started: 24 November 2026
© Author(s) 2026. CC BY 4.0 License.

series that reconciles inter-instrument differences between Dobson and Brewer instruments can enhance the robustness of satellite validation.

The long-term Arosa/Davos TCO time series, part of the Global Atmosphere Watch (GAW) network (Staehelin et al., 1998a), provides a unique observational basis for detecting long-term ozone changes in northern mid-latitudes (Rozanov et al., 2021). Initiated in 1926 at the Lichtklimatisches Observatorium (LKO) in Arosa, the time series constitutes the world's longest continuous TCO record (Staehelin et al., 1998a). Since 2011, the instruments have been carefully relocated to the Physikalisch-Meteorologisches Observatorium Davos and World Radiation Center (PMOD/WRC), with a 10-year overlapping measurement period to ensure the continuity of this historical record (Stübi et al., 2017, 2021)

During its 100-year history, the Arosa/Davos measurement objectives have been diverse: from the study of environmental factors in relation to medical recovery from tuberculosis, to its role in improving weather forecasts in the 1960s, the detection of ozone layer depletion at mid-latitudes during the 1980s, and more recently, the detection of its potential recovery (Staehelin et al., 2018; WMO, 2022). The Arosa TCO time series was homogenised in 1998 based primarily on Dobson observations, and various analyses have been conducted since then (Staehelin et al., 1998a, b; Scarnato et al., 2009, 2010; Stübi et al., 2017, 2021; Gröbner et al., 2021).

This TCO time series, composed currently of six collocated instruments providing quasi-simultaneous measurements, enables more reliable ozone monitoring, supports satellite product validation, and allows the investigation of past ozone levels and anomalies (Brönnimann, 2022).

This study is embedded within the Stratospheric and Tropospheric Ozone over the Alps and Europe (STOA) project and aims to develop a homogenised TCO series with a well-quantified uncertainty budget by merging six collocated Brewer and Dobson instruments covering the 1990–2024 period. This study period focuses on the regulation of ozone-depleting substances and the subsequent recovery phase. To ensure consistency across the entire record, we explicitly account for instrument relocation. Ultimately, this consistent TCO record, due to its high quality and robust characterization, is intended to serve as a benchmark dataset for long-term atmospheric ozone trends. The paper is organized as follows: The observation method and harmonisation methodology is presented in Section 2. The results are provided in Section 3, and the conclusions are drawn in Section 4.

2 Data and Methods

The homogenised time series is based on data merged from six collocated instruments: three Brewer and three automated Dobson spectrophotometers spanning the period from 1990 to 2024.

The Brewer triad consists of two single-monochromator MKII instruments, B040 and B072, and one double-monochromator MKIII instrument, B156. Brewer B040 began measurements in 1989, while Brewer B072 started operating in 1991. However, only data of B072 from 1995 onwards are used due to instrument malfunctions during the earlier period; therefore, reliable measurements are considered to start in 1995 (Stübi et al., 2017). The double-monochromator Brewer B156 has been operating since 1998.

The Dobson triad consists of instruments D101, D062, and D051. Dobson D101 began measurements in 1966. Dobson D062

https://doi.org/10.5194/egusphere-2026-6120
Preprint. Discussion started: 24 November 2026
© Author(s) 2026. CC BY 4.0 License.

has been operating continuously since 1992, while D051 was installed in 1956. It has been primarily used for Umkehr measurements (Götz et al., 1934; Petropavlovskikh et al., 2005; Maillard Barras et al., 2022) and since 2013 is measuring TCO, these measurements are not performed daily but are conducted periodically under optimal weather conditions, with a lower frequency during the winter months. A distinctive feature of this Dobson triad is its automated measurement system achieved in 2016, whereas most instruments across the global network remain manually operated. Technical details of this procedure are described by Stübi et al. (2021). This automation significantly increases the number of measurements performed daily and reduces the scatter of the values which was due to manual readout, thereby substantially improving the quality of the data record of the Dobson spectrophotometers. The availability of multiple instruments, together with continuous quality maintenance and calibrations, enables more robust monitoring of the total ozone column and facilitates the identification of systematic differences and instrumental drifts through intercomparison.

2.1 Total Column Ozone retrieval

2.1.1 Theoretical Framework

The Brewer and Dobson spectrophotometers retrieve total ozone column by performing direct solar irradiance (DS) measurements. These instruments track the sun to measure solar irradiance within the UV spectral range (310–340 nm), where ozone absorption is strong. The DS retrieval methodology is based on the Beer-Lambert law, which describes the attenuation of direct solar irradiance along the atmospheric path for a given optical depth (τ):

$$I(\lambda) = I_0(\lambda)e^{-\tau(\lambda)\mu} \tag{1}$$

Where I is the solar irradiance measured by the instrument, and I_0 is the solar irradiance at the top of the atmosphere. τ denotes the wavelength-dependent optical depth and μ is the corresponding airmass factor. The individual atmospheric extinction processes are described using specific effective airmass factors. In particular, μ_β represents the effective airmass for Rayleigh scattering, whereas μ_{O_3} represents that for ozone absorption.

To determine the total atmospheric attenuation at a specific wavelength, Eq. (1) can be rewritten as:

$$\tau(\lambda) = \frac{\ln I_0(\lambda) - \ln I(\lambda)}{\mu} \tag{2}$$

To isolate the specific contribution of ozone absorption within the 310–340 nm range, the attenuation caused by Rayleigh scattering (τ_β) must be subtracted from the total optical depth, yielding the ozone optical depth (τ_{O_3}) as follows:

$$\tau_{O_3}(\lambda) = \sigma(\lambda)X = \frac{\ln I_0(\lambda) - \ln I(\lambda) - \tau_\beta(\lambda)\mu_\beta}{\mu_{O_3}} \tag{3}$$

where $\sigma(\lambda)$ is the ozone absorption cross-section, the terms μ_β, μ_{O_3} and X correspond to the effective airmasses for Rayleigh scattering, ozone absorption, and TCO, respectively.

https://doi.org/10.5194/egusphere-2026-6120
Preprint. Discussion started: 24 November 2026
© Author(s) 2026. CC BY 4.0 License.

2.1.2 Instrumental Configurations and Weighting Schemes

Although both spectrophotometers share the same measurement principle, they differ in their optical design and sampling mechanisms; Brewer instruments measure solar irradiance quasi-simultaneously at four distinct wavelengths through a slit mask mechanism (λ_{1-4} : 310.1, 313.5, 316.8, and 320.0 nm) (Kerr et al., 1980, 1983, 1985) to retrieve TCO, whereas Dobson instruments measure the intensity ratios of two specific wavelength pairs by adjusting an optical wedge for each pair. Total column ozone is then retrieved from these measurements by specific weighting factors at each wavelength. The instrument-specific weighting coefficients (w_i) are defined as:

$$w_i^{\text{Brewer}} = [1,\ -0.5,\ -2.2,\ 1.7]$$
$$w_i^{\text{Dobson}} = [1,\ 1,\ -1,\ -1]$$

Both Dobson and Brewer spectrophotometers retrieve TCO using the so-called double-ratio technique, which combines measurements at four wavelengths as previously described. In this approach, the irradiance ratio is first calculated for each of the two wavelength pairs, followed by the determination of the ratio between these two quantities. While the Dobson algorithm applies weighting coefficients of equal magnitude, the Brewer algorithm uses specific weighting factors for each wavelength to minimize the combined effects of SO_2 interference, aerosol extinction, and wavelength shifts (Kerr et al., 1983, 1985; León-Luis et al., 2018). By combining measured irradiances, both algorithms largely cancel the constant and linear spectral contributions to atmospheric extinction, thus reducing aerosol interference and allowing ozone absorption to be more effectively isolated in the retrieval process (Dobson, 1957; Brewer, 1973; Kerr et al., 1980; Komhyr, 1980; Vanicek, 2006; Redondas et al., 2014; Gröbner et al., 2021; Zuber et al., 2021; Egli et al., 2023; Voglmeier et al., 2024).

Regarding the ozone absorption cross-section and the Rayleigh scattering would be rewritten in terms of their ozone absorption and Rayleigh coefficients, respectively. These quantities are obtained by weighting the spectral ozone absorption cross-sections and the spectral Rayleigh parametrization from Bodhaine et al. (1999) with the instrument's slit functions. The mathematical expressions and details of the calculation procedure are described in Gröbner et al. (2021). Accordingly, Eq.(3) can be rewritten as follows:

$$X = \frac{F_0 - F - \Delta\beta\mu_\beta}{\Delta\alpha\mu_{O_3}} \tag{4}$$

Here, F and F_0 denote the weighted sums of the natural logarithms of the measured and extraterrestrial (top-of-atmosphere, TOA) irradiances, respectively, whereas $\Delta\alpha$ and $\Delta\beta$ represent the differential ozone absorption and Rayleigh scattering coefficients. These quantities are defined as follows:

$$F = \sum_{i=1}^{4} w_i \ln I(\lambda_i), \quad F_0 = \sum_{i=1}^{4} w_i \ln I_0(\lambda_i), \quad \Delta\alpha = \sum_{i=1}^{4} w_i\alpha_i, \quad \Delta\beta = \sum_{i=1}^{4} w_i\beta_i. \tag{5}$$

The parameter F_0 corresponds to the extraterrestrial constant (ETC), an instrument-specific calibration parameter. For the Dobson and Brewer reference instruments, the ETC is determined using the Langley plot method at high-altitude calibration sites such as the Mauna Loa Observatory, Hawaii, or the Izaña Atmospheric Research Center, Canary Islands (Kerr et al.,

https://doi.org/10.5194/egusphere-2026-6120
Preprint. Discussion started: 24 November 2026
© Author(s) 2026. CC BY 4.0 License.

1980; Komhyr et al., 1989; León-Luis et al., 2018). The calibration of network instruments is then established through Brewer and Dobson intercomparison campaigns, during which the network instruments are compared with the corresponding standard reference instrument and their ETC values are determined relative to the reference. The Dobson reference instrument is operated by the Deutscher Wetter Dienst (DWD), whereas the Brewer reference triad is operated by the Izaña Atmospheric Research Center.

Since the accuracy of the ozone retrieval relies on instrumental stability, the ETC is continuously monitored via routine standard lamp (SL) tests, which reflects the stability and performance of the instruments (León-Luis et al., 2018).

2.2 Total Column Ozone Brewer dataset

The Brewer dataset was generated from the raw observational measurements, using the daily standard lamp tests to assess the stability of the instrument over time. The values of the standard lamp test as denoted as R6 values, which are directly related to the instrumental ETC by a constant C which is determined during the instrument calibration. Table 1 lists the ETC, R6, and the constant C value obtained from the RBCC-E campaigns organised biannually between 2008 and 2024.

From Table 1 the average relation C between the ETC and the standard lamps for the whole period are 1228, 1259, and 1304 units with standard deviations of 14, 7, and 9 units for B040, B072 and B156 respectively. These variabilities are similar to the calibration uncertainties of the RBCC-E campaigns and indicate that the R6 values from the standard lamp tests can be used to estimate the calibration constants ETC on a daily basis for the whole period of investigation.

Table 1. Comparison of ETC, R6 values, and C (ETC-R6) for instruments B040, B072, and B156 for different RBCC-E campaigns.

	Instument								
	B040			B072			B156		
Year	ETC	R6	C(ETC-R6)	ETC	R6	C(ETC-R6)	ETC	R6	C(ETC-R6)
2008	2960	1717	1243	3185	1920	1265	1750	435	1315
2010	2985	1745	1240	3168	1905	1263	1750	445	1305
2012	2985	1745	1240	3187	1925	1262	1765	458	1307
2014	2970	1740	1230	3223	1960	1263	1750	440	1310
2016	2950	1747	1203	3215	1960	1255	1740	445	1295
2018	2976	1742	1234	3221	1963	1258	1759	445	1314
2021	2972	1739	1233	3217	1949	1268	1761	453	1308
2022	2955	1742	1213	3200	1949	1251	1740	450	1290
2024	2960	1742	1218	3185	1940	1245	1745	450	1295
Summary $\overline{C} \pm \delta$ C			1228.2 ± 13.8			1258.9 ± 7.4			1304.3 ± 8.9

Discrete jumps in the R6 datasets of each Brewer due to standard lamp failures were taken into account in the derivation of the ETC datasets.

https://doi.org/10.5194/egusphere-2026-6120
Preprint. Discussion started: 24 November 2026
© Author(s) 2026. CC BY 4.0 License.

To account for the temporal evolution of the standard-lamp response, a fitting function was derived from the lamp measurements. A constant, linear, and second-order polynomial functions were used depending on the observed temporal behaviour. The fitted function was subsequently used to track the lamp stability and derive ETC values consistent with the measured evolution of the standard-lamp response.

Further instrument parameters, such as temperature correction coefficients and ozone absorption coefficients were taken from the RBCC-E calibration reports, which are shown in Table 2. The TCO for the whole period was then derived according to Eq. (4) using these coefficients.

Table 2. Temperature and ozone absorption coefficients configuration parameters for each Brewer instruments.

Instrument	Temperature coefficients	O_3 absorption coefficient
B040	-3.4690	0.3350
B072	-1.6200	0.3380
B156	-0.5190	0.3402 (2012-2015), otherwise 0.3410

Figure 1 shows the temporal evolution of the ETC values for the three Brewer instruments, providing an assessment of their long-term stability. Overall, the ETC values for B040 and B156 remain relatively stable throughout the measurement period. In particular, the large change observed for B156 in 2006 cannot be attributed to a documented standard-lamp replacement or a specific technical failure. No corresponding event was reported in the available instrument records; therefore, the cause of this abrupt variation remains unknown.

Before 1995, the B072 instrument was not functioning correctly and was sent back to the manufacturer for repairs. Therefore, measurements are only considered reliable from 1995 (Stübi et al., 2017). Figure 1 shows also a slight drift of the instrument between 2005 and 2011. As a drift in R6 values indicates a drift in instrument stability. This feature is corrected by using the R6 values to adjust the ETC.

Brewer observations were selected based on a standard deviation below 2.5 DU among simultaneous measurements, following the criteria adopted in the previous analysis by Stübi et al. (2017). Only for the single-monochromator Brewers, the air-mass range was restricted to values below 3.5, given their susceptibility to stray-light effects at high airmasses. This effect will be discussed in more detail in Section 2.2.2

2.2.1 Ozone absorption cross-section

The seasonal differences in TCO between Brewer and Dobson instruments have been widely reported in the literature (Kerr et al., 1988; Staehelin et al., 1998a; Kerr, 2002; Staehelin et al., 2003; Vanicek, 2006; Redondas et al., 2014; Köhler et al., 2018). Taking this into account, we followed the methodology presented by Gröbner et al. (2021) and Voglmeier et al. (2024) to harmonise the Brewer and Dobson observations.

https://doi.org/10.5194/egusphere-2026-6120
Preprint. Discussion started: 24 November 2026
© Author(s) 2026. CC BY 4.0 License.

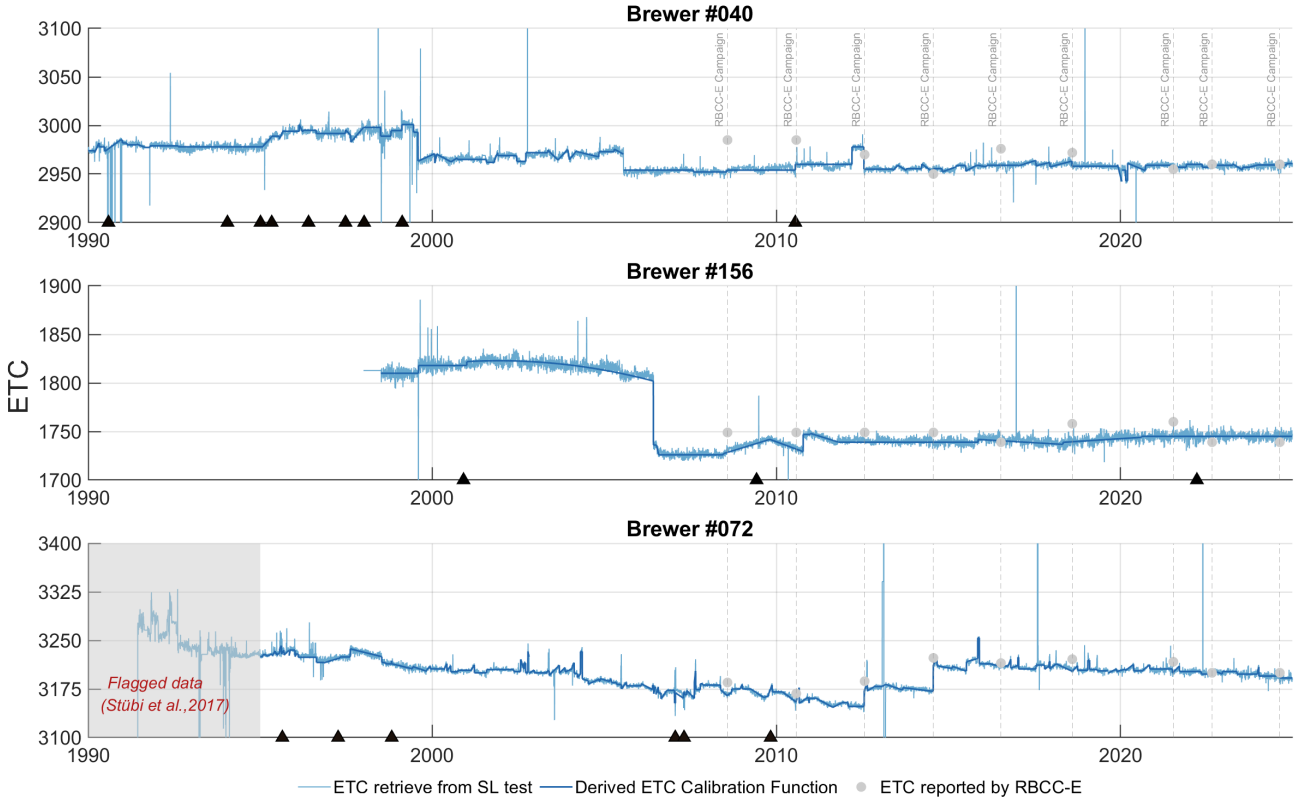

Figure 1. Time series of the extraterrestrial constant (ETC) for Brewer instruments B040 (top), B156 (middle), and B072 (bottom). The plots show ETC retrive from the R6 values (light blue), and the derived ETC calibrated function (dark blue). The gray-shaded area in the bottom panel highlights flagged data reported from Stübi et al. (2017). Black triangles mark standard lamp (SL) replacements, while grey filled circles represent the ETC derived during the respective RBCC-E campaigns.

The ozone absorption cross-sections in the UV are strongly dependent on the ozone effective temperature (T_{eff}), which is defined as the integrated atmospheric temperature weighted with the ozone profile along the atmospheric column. Under the framework of the Integrated Global Atmospheric Chemistry Observation (IGACO) program of the World Meteorological Organization (WMO) (https://igaco-o3.fmi.fi/ACSO/index.html), efforts focused on the investigation of different ozone absorption cross-sections and of their temperature dependence in order to replace the operational ozone absorption cross-section by Bass and Paur (1985). The ozone absorption cross-section measured at the University of Bremen (Serdyuchenko et al., 2014), referred to as SG16, shows a better performance than other available ozone absorption cross-sections, and significantly reduces the seasonal differences between Dobson and Brewer instruments, as highlighted by Redondas et al. (2014) and Gröbner et al. (2021).

To implement the SG16 ozone cross-section, we used the following equation by Voglmeier et al. (2024):

https://doi.org/10.5194/egusphere-2026-6120
Preprint. Discussion started: 24 November 2026
© Author(s) 2026. CC BY 4.0 License.

$$X(T_{\text{eff}}) = X_{\text{OP}} \frac{\Delta\sigma_{\text{OP}}(T_{\text{OP}})}{\Delta\sigma(T_{\text{eff}})} \tag{6}$$

where $X(T_{\text{eff}})$ denotes the retrieved TCO using the Serdyuchenko ozone absorption cross-sections calculated for a specific effective ozone temperature, while X_{OP} denotes the TCO retrieved using the operational Bass and Paur ozone absorption cross-sections at a fixed temperature, T_{OP}, is -45°C for Brewer and -46.3°C for Dobson instruments. $\Delta\sigma_{\text{OP}}$ and $\Delta\sigma_{T_{\text{eff}}}$ are the differential operational ozone absorption cross-section (Bass and Paur, 1985) and the differential ozone absorption cross-section measured at the University of Bremen (Serdyuchenko et al., 2014), respectively.

Kerr (2002); Staehelin et al. (2003); Vanicek (2006); Scarnato et al. (2009); Redondas et al. (2014), and Orphal et al. (2016) investigated the effects of the ozone absorption cross-section, identifying it as a primary contributor to the discrepancies observed between Brewer and Dobson instruments. Scarnato et al. (2009) showed that the accuracy of TCO observations is limited by the uncertainty of ozone absorption cross-sections measured by different international laboratories. As shown by Gröbner et al. (2021), the Brewer instruments exhibit a negligible effective ozone temperature dependency when the ozone absorption cross section from Serdyuchenko et al. (2014) is used.

In addition to the ozone absorption cross-section, the Rayleigh scattering coefficient β is taken into account, as described in Eq.(4). For this purpose, the Rayleigh coefficients from Bodhaine et al. (1999) were applied to the Brewer dataset, resulting in approximately $\Delta\beta = 0.82$ and $\Delta\beta = 0.80$ for Davos and Arosa, respectively.

2.2.2 Single Brewer Stray Light

In contrast to double monochromator spectrophotometers, single monochromator Brewer instruments are substantially affected by internal stray light (SR). For the single monochromator Brewers, B040 and B072, the stray light effect becomes significant at high solar zenith angles (low solar elevation), which are common under winter conditions in Arosa and Davos. Following Redondas et al. (2021), this relationship can be parametrized as:

$$X_{\text{cor}} = X - \frac{a(\text{OSC})^b}{\Delta\alpha\mu} \tag{7}$$

Where X_{cor} and X correspond to the corrected and operational total column ozone, respectively; a and b are empirical coefficients for each instrument determined by comparison to the reference double monochromator Brewer of the RBCC-E; OSC stands for the ozone slant column defined as the product of TCO and the airmass (μ) and, $\Delta\alpha$ denotes the differential ozone absorption coefficient.

For the stray-light correction, the coefficients from the three most recent RBCC-E campaigns were considered, as none of the individual campaign results was considered more representative and the standard deviation of the campaign-derived coefficients is included as an indication of their variability (shown in Table 3).

The stray light correction was determined for each set of coefficients as a function of the ozone slant column described as $a(\text{OSC})^b$ in Eq (7). The corrections were then averaged at each ozone slant column, and the resulting average correction

https://doi.org/10.5194/egusphere-2026-6120
Preprint. Discussion started: 24 November 2026
© Author(s) 2026. CC BY 4.0 License.

values were fitted using the same functional form. These yielded representative coefficients of $a = -20.3$ and $b = 3.8$ for B040 and $a = -32.7$ and $b = 3.44$ for B072.

Table 3. Empirical a and b coefficients for the B040 and B072 from RBCC-E campaigns between 2018 and 2022.

	B040		B072	
Year	a	b	a	b
2018	-9.0	5.5	-17.4	3.8
2021	-10.2	5.2	-27.8	3.9
2022	-27.0	3.6	-42.0	3.3
Summary	-15.4 $\pm$ 10.1	4.8 $\pm$ 1.0	-29.1 $\pm$ 12.3	3.7 $\pm$ 0.3

2.3 Total Column Ozone Dobson dataset

The TCO datasets of the Dobson spectrophotometers are obtained following a similar procedure as for the Brewer spectrophotometers, using standard lamp tests to check and, if necessary, correct the ETC values in case of instrumental changes. In contrast to the Brewer spectrophotometers, fixed nominal ozone absorption coefficients are used assuming that the optical characteristics of all Dobson spectrophotometers are equal. As shown in Gröbner et al. (2021), and Köhler et al. (2018), this is not strictly correct, and can result in airmass dependencies of the TCO. Measurements characterizing the individual instrument wavelength settings are available only from 2018 onward. Since these measurements are directly related to the effective wavelength positions used for TCO retrieval, the corresponding absorption coefficients cannot be reliably reconstructed for earlier periods and therefore are not included in this study.

With respect to the wavelength pair used for TCO retrieval, only the AD pair was considered in this study, as it is generally considered the most reliable wavelength pair for Dobson measurements (Komhyr, 1980; Vanicek, 2006). For the measurements performed with the Dobson instrument, no constraint related to stray light was applied.

As discussed in Section 2.2.1, the TCO retrievals from Dobson instruments are significantly influenced by the effective ozone temperature. To account for this influence, the ozone absorption coefficients were calculated using the effective ozone temperatures T_{eff}, which were obtained by integrating the ozone density O_3 and temperature $T(z)$ profiles from the ozone sonde profiles from the Federal Office of Meteorology and Climatology (MeteoSwiss) in Payerne. Due to the sonde's burst height around $\sim$ 30 km, the ozone and temperature above the burst level are estimated by linear interpolation with the measured profiles with standard values from the U.S. Standard Atmosphere (NOAA, 1976), which considers a profile from the surface up to 120 km in the atmosphere. The relationships between these quantities are described by the following equation:

$$T_{\text{eff}} = \frac{\int T(z)\mathrm{O}_3(z)\,dz}{\int \mathrm{O}_3(z)\,dz} \tag{8}$$

Where z indicates the altitude with respect to the surface. The integral covers the whole atmospheric column, from the surface to the top of the atmosphere at 120 km. Subsequently, we developed an effective ozone temperature time series using

https://doi.org/10.5194/egusphere-2026-6120
Preprint. Discussion started: 24 November 2026
© Author(s) 2026. CC BY 4.0 License.

the ozone sonde measurements as a baseline. Additionally, in order to fill gaps between ozone sonde launches (typically occurring three times per week), the daily effective ozone temperature from the Tropospheric Emission Monitoring Internet Service (TEMIS) was included when no ozone sonde data were available. Further details on the dataset are provided by Van der A et al. (2010), while the effective ozone temperature data for Arosa/Davos are available through the TEMIS website (https://www.temis.nl/climate/efftemp/overpass.php, Location: Arosa).

To ensure consistency between both data sources, the TEMIS data were calibrated relative to the ozone sonde dataset using a linear regression. A comparison between the effective ozone temperatures from the sondes and TEMIS retrievals showed a strong correlation ($r^2 = 0.98$), and their relationship is given by:

$$T_{\mathrm{O_3sonde}} = 1.05 \cdot T_{\mathrm{TEMIS}} + 0.82°C \tag{9}$$

In line with this approach, the equation was applied to the TEMIS dataset to estimate the effective ozone temperature when ozone sonde data were unavailable. Furthermore, a sensitivity test demonstrated that the impact of using TEMIS data instead of the ozone sonde data did not exceed 0.1% in TCO. Figure 2 shows the effective ozone temperature time series, red dots

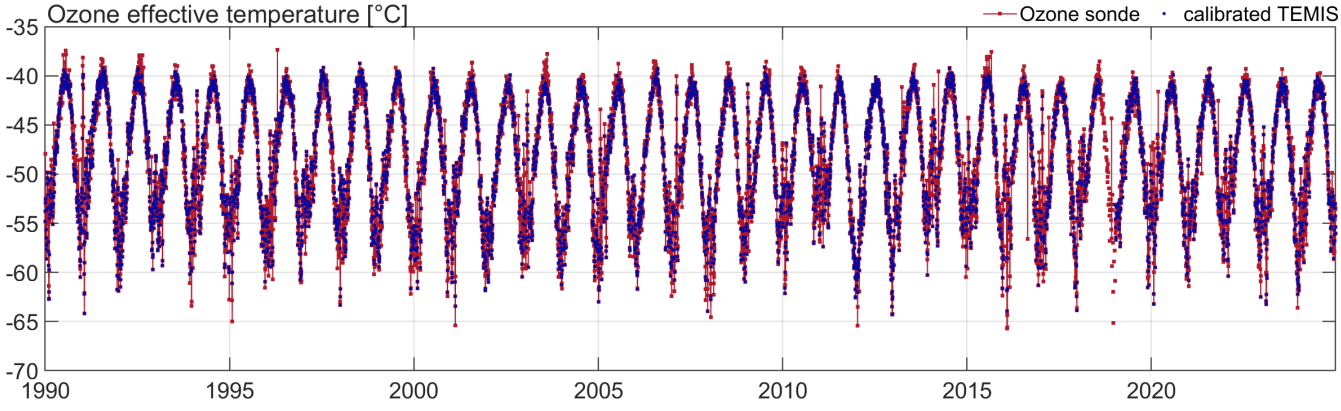

Figure 2. Effective ozone temperature timeseries (1990–2024) obtained from ozone sonde measurements (red dots) and the TEMIS dataset (blue dots). The red dots indicate the available data from ozone sonde and blue dots the TEMIS data utilized and calibrated relative to the ozone sonde measurements.

indicate the observations from ozone sonde, while blue dots illustrate the measurements obtained from TEMIS and calibrated using Eq. (9).

Similarly to the Brewer procedure, the ozone absorption coefficients used for the ozone retrieval of the Dobson spectrophotmeters were converted from the operational (Bass and Paur, 1985) ozone absorption cross-sections to the Serdyuchenko cross-sections following the approach described in Voglmeier et al. (2024) and the reference therein:

$$\alpha(T_{\mathrm{eff}}) = A_0(\lambda) + A_1(\lambda)T_{\mathrm{eff}} + A_2(\lambda)T_{\mathrm{eff}}^2 \tag{10}$$

Where A_0, A_1 and A_2 are the coefficients from Serdyuchenko et al. (2014), as shown in Table 4. of Voglmeier et al. (2024), and $\alpha(T_{\mathrm{eff}})$ is the ozone absorption coefficient for a given ozone effective temperature.

https://doi.org/10.5194/egusphere-2026-6120
Preprint. Discussion started: 24 November 2026
© Author(s) 2026. CC BY 4.0 License.

2.4 Uncertainty Budget

2.4.1 Brewer Uncertainty

To determine the TCO uncertainty, we focused on the instrument-specific uncertainties of the Brewer spectrophotometers. For this purpose, we considered the most relevant parameters from Eq. (3), such as ETC, F, P, $\Delta\alpha$ and the stray light. Using the methodology presented in Redondas et al. (2020) and the Guide to the Expression of Uncertainty in Measurement (GUM) (JCGM, 2008), these coefficients are represented by the partial derivatives with respect to each component. The uncertainty components were then obtained for each parameter by multiplying it with the estimated parameter uncertainty as shown in Table 4.

The uncertainty of the ETC parameter depends on its correlation with the R6 values used to determine the constant C listed in Table 1 which implicitly also takes into account the uncertainty in the calibration by the reference Brewer during the RBCC-E. The average estimated uncertainty of ETC as shown in Table 1 is 13.8, 7.4, and 8.9 for B040, B072 and B156 respectively. Due to the small differences between the three instruments, a common uncertainty of 10 units was chosen for the ETC parameter when calculating the combined uncertainty of the datasets.

In the Brewer and Dobson algorithms only a constant climatological value for the ambient pressure is used. Therefore, the uncertainty in the ambient pressure used for the TCO retrieval was based on the standard deviation of the pressure measurements from the Automatic Weather Stations (AWS) operated by MeteoSwiss in Davos and Arosa. Assuming a normal distribution yields a pressure uncertainty of ± 7 mbar, in line with Egli et al. (2022).

The ozone absorption coefficient depends on the grating orientation, which is controlled by a micrometer in the instrument; small changes in the micrometer will result in a change in wavelength and correspondingly, a change in the ozone absorption coefficient, denoted as α_{step} in Table 4. The smallest wavelength change is 0.0075 nm, corresponding to a change of one step of the micrometer. During the characterization of the wavelength dispersion of the Brewer spectrophotometer, ozone absorption coefficients are calculated for different positions of the micrometer, resulting in a change in ozone absorption coefficient of $\sim 0.3\%$ for a one step change in the micrometer (Redondas et al., 2018). In table 4, the sensitivity parameter is simply the derivative from Eq.(4). The instrumental uncertainty is then calculated by multiplying the parameter's uncertainty by the derivative.

The remaining instrument-specific contributions considered here are the measurement repeatability associated with F and the effect of stray light considered with a different approach. The uncertainty associated with F was estimated from the repeatability of four consecutive TCO measurements. Each measurement cycle comprises 20 observations, with each observation consisting of four consecutive TCO measurements. A measurement cycle was considered valid when the standard deviation of the four wavelength measurements was ≤ 2.5 DU. The corresponding maximum uncertainty associated with measurement repeatability was therefore estimated as $\frac{2.5}{\sqrt{4-1}} = 1.4$ DU.

For the single-monochromator Brewer spectrophotometers, the contribution of stray light was also included in the TCO uncertainty. The variability in the empirical coefficients obtained from the different RBCC-E campaigns results in a range of stray light correction values that depends on the ozone slant column. A representative correction values was determined as we

https://doi.org/10.5194/egusphere-2026-6120
Preprint. Discussion started: 24 November 2026
© Author(s) 2026. CC BY 4.0 License.

Table 4. Sensitivity coefficient for the TCO retrieval. β corresponds to the Rayleigh coefficients. μ_β and μ is the Rayleigh airmass and the airmass. P_0 is the standard pressure. $\Delta\alpha_{\text{step}}$ is the change in the ozone differential absorption coefficient in one step and α corresponds to the differential ozone absorption coefficient.

Parameter	Sensitivity Coefficient	Instrumental Uncertainty
ETC	$\frac{1}{\alpha\mu}$	10 units
P	$\frac{\beta\mu_\beta}{\alpha\mu p_0}$	7.0 mbar
α	$-\frac{X\,\Delta\alpha_{\text{step}}}{\Delta\alpha}$	0.0075 nm

describe in Section 2.2.2, and the uncertainty associated with the stray light correction was estimated as the deviation bounded by the minimum and maximum correction values obtained from the range of a and b coefficients. Consequently, the magnitude of the uncertainty varies with the ozone slant column, reflecting the dependence of the stray light correction on this parameter. Ultimately, the contributions of the individual uncertainty components for one measurement performed by the instrument were combined to obtain the overall measurement uncertainty, as follows:

$$u^2 = C_{\text{ETC}}^2 u_{\text{ETC}}^2 + C_{\text{F}}^2 u_{\text{F}}^2 + C_{\text{P}}^2 u_{\text{P}}^2 + C_\alpha^2 u_\alpha^2 + u_{\text{SR}}^2 \tag{11}$$

Where u corresponds to the combined uncertainty; $C_{\text{ETC}}u_{\text{ETC}}$, $C_{\text{F}}u_{\text{F}}$, $C_{\text{p}}u_{\text{p}}$ and $C_\alpha u_\alpha$ denote the products of the sensitivity coefficient and their respective instrumental uncertainty for the ETC, the measurement, the pressure and the ozone absorption coefficient, and u_{SR} is the stray light uncertainty. The daily mean TCO is obtained as a weighted average of the individual ozone measurements, with weights given by the inverse of their squared uncertainties. The resulting combined uncertainty values are shown in black in Figs. 3a, 3b, and 3c. This overall shape of the uncertainty evolution remains consistent throughout the dataset.

To estimate a representative uncertainty for each daily mean TCO, the correlation between the individual uncertainty components within a given day must be considered. Uncertainty components associated with the ETC, ambient pressure, and stray light correction are treated as correlated among the measurements performed on the same day. Therefore, these contributions are not reduced by the number of measurements. In contrast, the measurement uncertainty and the uncertainty associated with the ozone absorption coefficient, arising from the wavelength setting uncertainty, are considered uncorrelated between individual measurements. Their contributions, as described by Eq. (11), are therefore reduced according to the number of measurements (N).

Figure 3 shows the uncertainty components for the Brewer instruments, expressed as percentages. Among the uncertainties derived from the TCO retrieval (See Table 4), the dominant contribution comes from the ETC. The measurement parameter and the ozone absorption coefficient contribute equally, in terms of magnitude, to the uncertainty budget. Regarding the pressure, its contribution is on the order of 10^{-7} DU, which is negligible compared to that of the other variables. It is important to

https://doi.org/10.5194/egusphere-2026-6120
Preprint. Discussion started: 24 November 2026
© Author(s) 2026. CC BY 4.0 License.

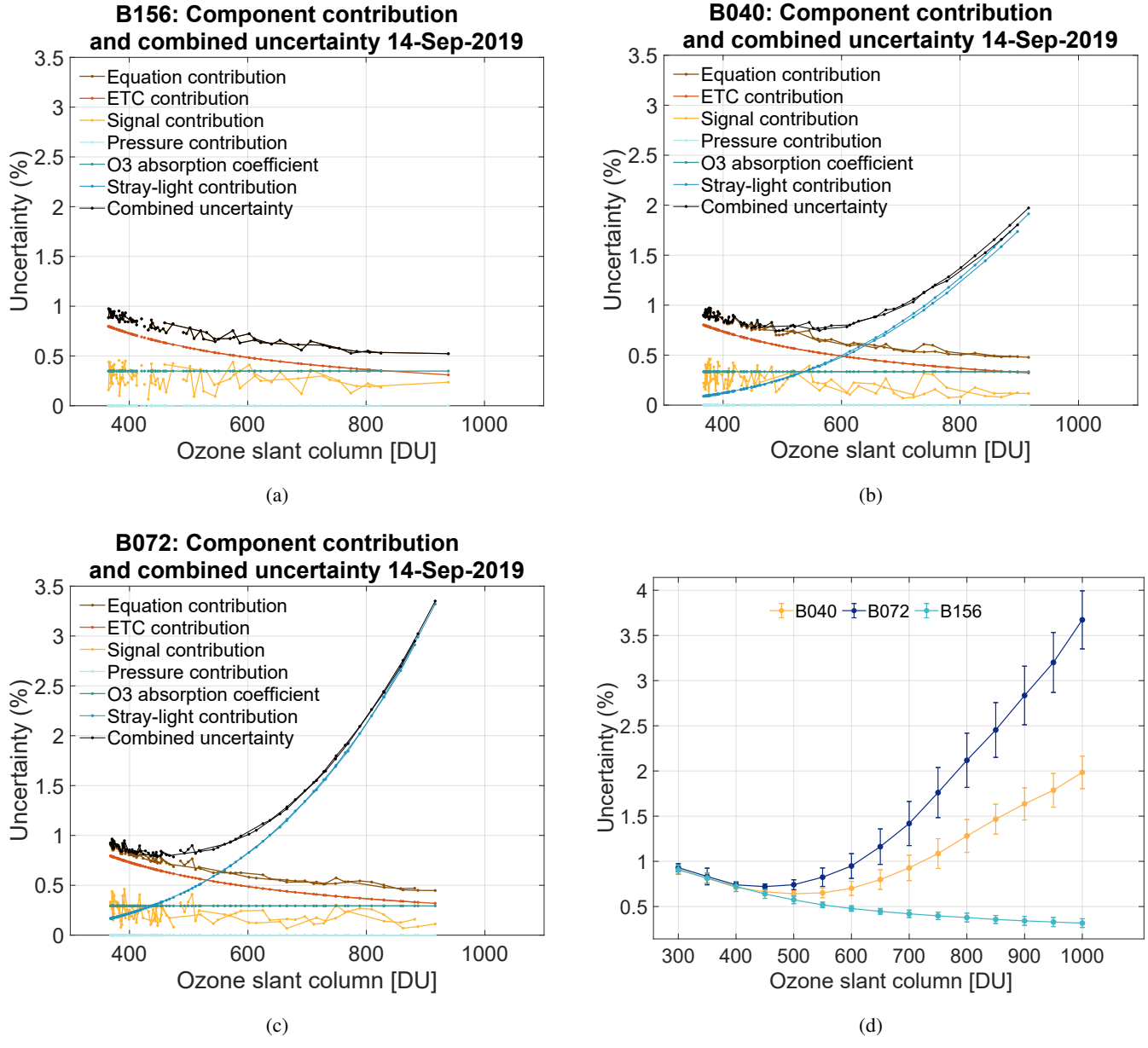

Figure 3. Combined uncertainty and individual uncertainty components for measurements performed under airmass conditions ($\mu \leq 3.5$) on 14 September 2019 for (a) Brewer #156, (b) Brewer #040, and (c) Brewer #072. (d) Relative combined uncertainty for the B040, B072, and B156 instruments.

note that for the single monochromator Brewers (B040 and B072), the uncertainty starts to be dominated by the stray light contribution at an ozone slant column of about 600 DU. Comparing Figures 3b and 3c, Brewer B072 exhibits a larger stray light effect, as its uncertainty increases more rapidly than that of B040. To further characterize the measurement performance,

https://doi.org/10.5194/egusphere-2026-6120
Preprint. Discussion started: 24 November 2026
© Author(s) 2026. CC BY 4.0 License.

the relative uncertainties of the three instruments are shown as a function of ozone slant column in Fig.3d. The uncertainty at each slant-column interval is represented by the standard deviation of the measurements within 50-DU bins. The uncertainty values for the Brewer triad remain similar up to 600 DU. By contrast, the uncertainties associated with single-monochromator Brewers (B040 and B072) are larger at higher ozone slant path values, which makes the differences between them and B156 more pronounced.

Table 5. Contribution of each parameter to the relative uncertainty (%) per individual instrument for the measurements performed under airmass conditions $\mu = 2$ and $\mu = 3$ on 14th September 2019.

Instrument B040	Uncertainty (%)					
	ETC	F	P	α	SR	Combined Uncertainty (u)
$\mu = 2$	0.54	0.39	$7.8 \cdot 10^{-7}$	0.33	0.36	0.83
$\mu = 3$	0.37	0.08	$8 \cdot 10^{-7}$	0.33	1.28	1.36
Instrument B072	Uncertainty (%)					
	ETC	F	P	α	SR	Combined Uncertainty (u)
$\mu = 2$	0.54	0.12	$7 \cdot 10^{-7}$	0.29	0.59	0.86
$\mu = 3$	0.37	0.27	$7.9 \cdot 10^{-7}$	0.29	2.02	2.09
Instrument B156	Uncertainty (%)					
	ETC	F	P	α	SR	Combined Uncertainty (u)
$\mu = 2$	0.55	0.35	$7.8 \cdot 10^{-7}$	0.35	-	0.74
$\mu = 3$	0.36	0.19	$7.8 \cdot 10^{-7}$	0.35	-	0.54

To account for the contribution of each component to the relative combined uncertainty, TCO measurements for airmasses $\mu = 2$ and $\mu = 3$ were selected as illustrative examples. The relative uncertainty of each parameter in Eq.(11) with respect to the TCO value calculated in percent, and presented in Table 5. These results show comparable contributions from F, ETC and α to the combined uncertainty for each instrument. The largest differences between instruments were caused by the stray light contribution in the B040 and B072.

2.4.2 Dobson Uncertainty

The uncertainty of TCO measurements obtained with a Dobson spectrophotometer depends strongly on the stability of its calibration and optical characteristics. According to the WMO Dobson Operations Handbook (Komhyr, 1980) changes in instrument spectral response were monitored primarily through mercury-lamp and standard-lamp tests – similar to the stability test of the Brewers using the standard lamp and mercury lamp (see Section 2.2) - and periodic comparisons with WMO dedicated reference instruments. Periodic intercomparison on a five to six year schedule with the reference Dobson D064, from the Deutscher Wetterdienst (DWD) at Hohenpeissenberg, Germany, provides an empirical assessment and assurance of the measurement quality for D051, D062 and D101. The intercomparison results after calibration demonstrated agreement for

https://doi.org/10.5194/egusphere-2026-6120
Preprint. Discussion started: 24 November 2026
© Author(s) 2026. CC BY 4.0 License.

the operational AD ozone product of all three instruments, within less than 0.5% compared to the reference. These values, however, should be interpreted as intercomparison variability rather than complete measurement uncertainty. A formal overall uncertainty budget for each individual instrument requires the assessment of the uncertainty of the wavelength calibration and its effect on the ozone absorption coefficient, the measurement from the automatic readings, the wedge calibration, the variability of the standard and mercury-lamp tests and their correlations and dependencies. A recent Monte-Carlo simulation using all instrumental readings of the automated Dobsons, wedge calibration results and slit function measurements with the portable tuneable radiation source TuPS (Smid et al., 2021) from the regional Dobson intercomparison in 2024 in Davos, and weekly lamp tests, revealed an overall instrument uncertainty of all three Dobsons of around 1% accross all ozone slant paths. For generating a detailed study on the overall uncertainty from the Arosa/Davos Dobson triade describing all relevant parameters of uncertainty and the applied Monte-Carlo simulation will be addressed in a separated publication.

2.5 Instrument relocation from Arosa to Davos

Arosa and Davos share geographical similarities. Both sites are located above the Swiss Plateau inversion layer and feature a similar number of days per year on which the instruments perform direct sun measurements (∼300 days). Their horizons are also comparable, with minor differences occurring only at the extreme east and west during the summer months, as shown in Fig. 2 of Stübi et al. (2017). Although industrial activity is more developed in Davos than in Arosa, it remains highly limited. Furthermore, the PMOD/WRC sits above a well-pronounced inversion layer, which effectively prevents local valley pollution from reaching the observatory (Stübi et al., 2017).

The relocation of the instruments from Arosa to the nearby Davos valley (13 km aerial distance and 260 m altitude difference) between 2011 and 2021 was a major challenge due to the risk of a disruption in the world's longest ozone time series. Therefore, a 10-year transition period was established, during which individual instruments from the two triads were alternately operated at the two locations. Figure 4 illustrates the measurement timeline at both locations, highlighting the 10-year transfer period of the instruments.

The intercomparison analysis between both sites is detailed in Stübi et al. (2017, 2021). In this study, we reanalyse the instrument relocation, using the harmonised datasets of the Brewer and Dobson spectrophotometer as described in the previous sections.

For the intercomparison between these sites, we compared B072 against B040, and D101 against D062 as well as the merged Dobson and Brewer datasets at each station. The latter comparison required the harmonisation of the Dobson and Brewer TCOs using the procedure outlined previously and extends the comparison published by Stübi et al. (2017). B072 and D101 were chosen for comparison because they were the first instruments transferred to Davos, whereas B040 and D062 were the last ones relocated. We used synchronized measurements within a 5-minute time window for the analysis. The systematic differences between the instruments when both measured either in Arosa or Davos were quantified and taken into account in the comparison to better assess the impact of the site relocation. To ensure representative measurements throughout the year, only observations within the ozone slant column range of 850–950 DU were selected. Different airmass or slant column ranges would not have provided a temporally homogeneous sampling across the whole year.

https://doi.org/10.5194/egusphere-2026-6120
Preprint. Discussion started: 24 November 2026
© Author(s) 2026. CC BY 4.0 License.

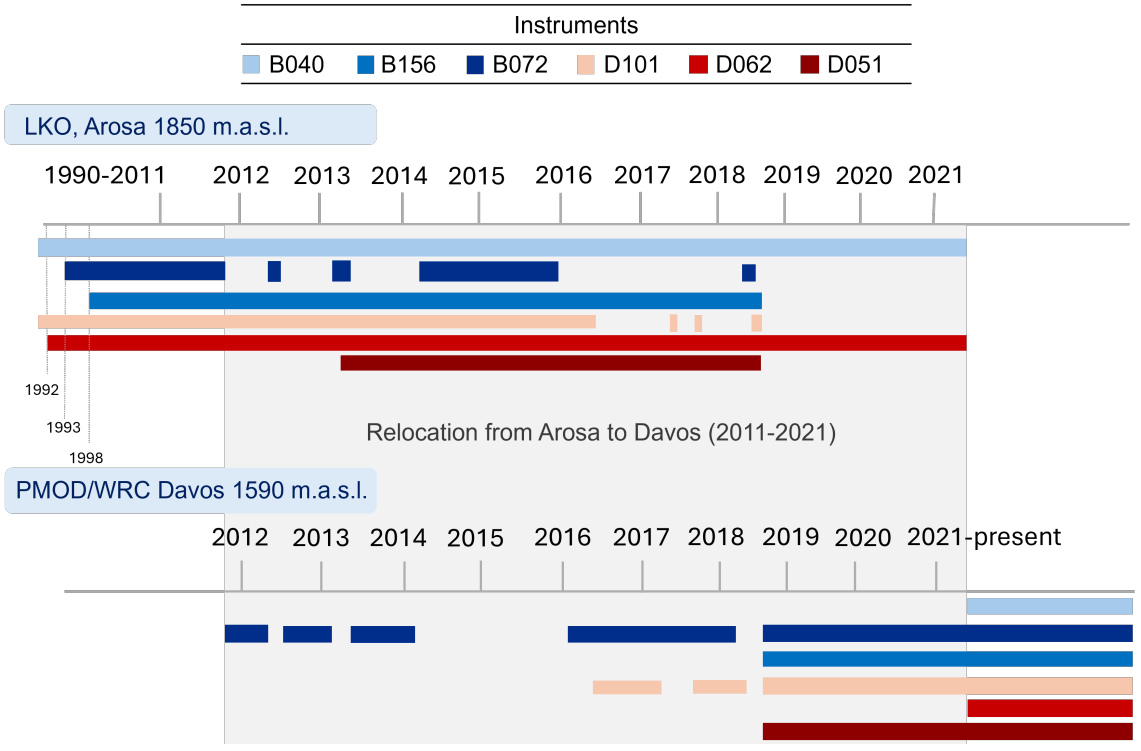

Figure 4. Timeline of the instruments relocation between Arosa (LKO) and Davos (PMOD/WRC) stations from 1990 to the present. Horizontal bars indicate the operational periods for the individual Brewer (blue gradients) and Dobson (red gradients) spectrophotometers. The shaded grey area illustrates the relocation phase between 2011 and 2021.

The relative monthly mean differences between the Brewer and Dobson instruments were used to assess the climatological differences in TCO between Arosa and Davos.

Figure 5 illustrates the monthly mean relative differences between Davos and Arosa. Figure 5 shows no clear seasonal variability, while the median of the combined instruments distribution, produced by a conventional mean between two datasets (shown in yellow, $0.33\% \pm 0.78\%$), is comparable in magnitude to the climatological differences in the tropospheric ozone column associated with the 260 m height difference (represented by the grey dashed line in Figure 5), as described below.

To complement this analysis, we evaluated surface ozone concentrations. In Arosa, these measurements were conducted by the Amt für Natur und Umwelt (ANU) of the Canton of Graubünden. In Davos, surface ozone concentrations are monitored as part of the National Air Pollution Monitoring Network (NABEL) in Switzerland. We analysed the differences in surface ozone concentration from 2006 to 2020, finding average concentrations of 39.6 ± 11.0 ppb for Arosa and 39.19 ± 11.2 ppb for Davos. In terms of DU, the differential ozone content between Arosa and Davos was calculated using Eq. (12):

https://doi.org/10.5194/egusphere-2026-6120
Preprint. Discussion started: 24 November 2026
© Author(s) 2026. CC BY 4.0 License.

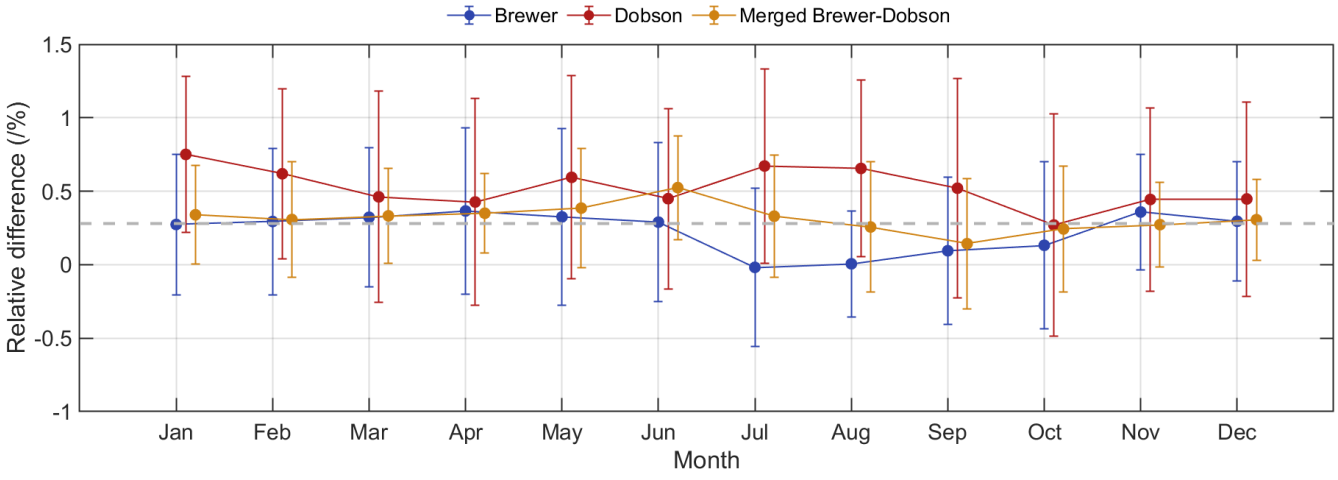

Figure 5. a) Relative differences in TCO measurements obtained from Brewer (blue), Dobson (red) and merged instruments (yellow) between Davos and Arosa. The grey dashed-line indicates the difference in the tropospheric ozone column between Davos and Arosa ($0.28\% \pm 0.13\%$).

$$\mathrm{O}_{3,\mathrm{content}} = 0.789 \int_{p_{\mathrm{arosa}}}^{p_{\mathrm{davos}}} \mathrm{O}_{3,\mathrm{ppm}} dP \tag{12}$$

where $\mathrm{O}_{3,\mathrm{content}}$ corresponds to the ozone content in DU. The $\mathrm{O}_{3,\mathrm{ppm}}$ is the surface ozone concentration in parts per million, and p_{arosa} and p_{davos} represent the atmospheric pressure at the Arosa and Davos stations, respectively. The detailed derivation of this conversion is provided in the appendices of Ziemke et al. (2001, 2003).

As no ozone profile was available within the column between Davos (840 hPa) and Arosa (812 hPa), three scenarios were explored in order to derive the ozone content within this column: the first considered the Arosa ozone concentration (39.6 ppb); the second used the concentration measured in Davos (39.2 ppb); and the third adopted the average mixing concentration from both stations (39.4 ppb). The monthly relative difference was calculated with the ratio between the ozone content using Eq.(12) and the daily TCO. In total, each monthly mean was computed using 15 months representative of the period from 2006 to 2020. Our findings show no indication of a change in TCO differences over this period, establishing an average contribution of $0.28 \pm 0.13\%$ to the difference in the tropospheric column associated with 260 m altitude difference. This shows good agreement with the previous analysis (Figure 5). Based on these results, we propose a constant transfer function, equal to the tropospheric ozone column difference ($0.28 \pm 0.13\%$), to convert Arosa TCO measurements to Davos-equivalent values, consistent with the findings of Stübi et al. (2017).

https://doi.org/10.5194/egusphere-2026-6120
Preprint. Discussion started: 24 November 2026
© Author(s) 2026. CC BY 4.0 License.

3 Results

3.1 Total Column Ozone composite derivation

In previous studies the homogenisation and analysis of the Arosa TCO time series were based on Dobson measurements (D02, D07, D015 and D101) only, and attempts to reconcile the Brewer and Dobson data focused primarily on proposing statistical transfer functions to convert Brewer measurements using the Dobson record as a reference (Staehelin et al., 1998a; Scarnato et al., 2010). This work presents the first fully homogenised record based on merged Brewer and Dobson observations for the Arosa/Davos location.

To produce a homogenised dataset from measurements obtained with different instruments, whether satellite or ground-based, periods of overlap during which the instruments operate simultaneously can be used to assess inter-instrument differences and to identify potential bias, drifts, and instrumental artefacts (Staehelin et al., 1998a; Fioletov et al., 2002). These overlapping observations provide a basis for correcting differences between successive datasets and for ensuring consistency throughout the resulting time series.

Different approaches have been developed to merge different ozone datasets and to estimate the uncertainty of the resulting composite. For example, Ball et al. (2017) developed the BASIC approach, a Bayesian statistical framework that combines different ozone composites while accounting for instrumental artefacts and drifts. The method incorporates uncertainties associated with the monthly input composites and monthly transition periods to derive an uncertainty for the resulting ozone composite. On the other hand, Bodeker et al. (2021) homogenised multiple satellite-based TCO datasets using corrections derived from comparisons with ground-based Dobson and Brewer measurements. The corrected datasets were subsequently combined using an uncertainty-weighted mean, with the weights determined from the uncertainties of the individual measurements. This approach produces a daily TCO dataset and propagates the measurement and correction uncertainties to the final composite product. The latter approach is therefore more closely aligned with the methodology adopted in this investigation.

In this study, we followed the consensus values and weighting scheme proposed by Paule and Mandel (1982, 1989) to merge the datasets from the six collocated instruments. This method provides the best estimate of TCO and its uncertainty as a weighted average of the quasi-simultaneous measurements from Brewer and Dobson, with the weights being the calculated uncertainties of each instrument.

Additionally, the modified Z-score proposed by Iglewicz and Hoaglin (1993) was used for outlier treatment on a daily scale, defined as:

$$Z = 0.6745\left(\frac{X - \text{Median}}{\text{MAD}}\right) \tag{13}$$

where MAD is the median absolute deviation from the mean, the constant value 0.6745 comes from $E(MAD) = 0.6745\sigma$, which is a rescaling factor for normally distributed data and X corresponds to the TCO.

The modified Z-score was preferred over the conventional Z-score as it relies on the median and median absolute deviation, whereas the conventional Z-score is based on the mean and standard deviation. The median and MAD are more robust to

https://doi.org/10.5194/egusphere-2026-6120
Preprint. Discussion started: 24 November 2026
© Author(s) 2026. CC BY 4.0 License.

outliers than the mean and standard deviation, respectively. Daily mean observations with a modified Z-score greater than 3.5 ($Z > 3.5$), corresponding to a probability threshold beyond 3σ, were excluded from the dataset.

When observations from a single instrument were available on a given day, that instrument provided the basis for the corresponding daily TCO estimate. These resulting daily values generally have larger uncertainties than those derived from observations from multiple instruments

Additionally, isolated measurements exhibiting elevated TCO values were identified, for which no observations were available on the preceding and following day, using ancillary meteorological data from MeteoSwiss (available at https://opendatadocs.meteoswiss.ch/a-data-groundbased/a1-automatic-weather-stations). These cases were examined and found to correspond to days with short sunshine duration (< 1 h), associated with overcast conditions. Therefore, the direct sun measurement was not performed under optimal conditions and these measurements (n = 37) were excluded from the dataset. Furthermore, daily means with uncertainties larger than 30 DU ($\sim 10\%$), mainly correspond to measurements associated with days when only one or two instruments were available and less than 10 observations were acquired, thus 55 days were excluded from the dataset.

The homogenised time series spans 1990–2024 and covers 90% of the total data period (12,784 days). The associated measurement uncertainty is characterized by 25th and 75th percentiles of 1.3 and 2.2 DU, respectively. No particular period of large TCO uncertainty was identified between 1990 and 2024 indicating the overall good quality of the measurements. Days with higher uncertainty did not persist for more than two consecutive days, occurring only sporadically throughout the time series.

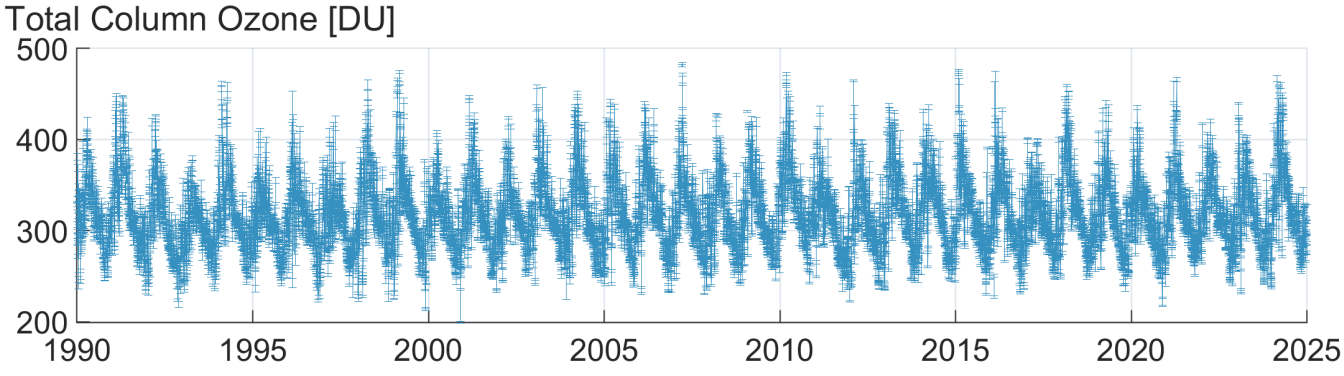

Figure 6. Homogenised TCO daily means of the Arosa/Davos record covering the 1990 to 2024 period. Error bars show the daily uncertainties of the composite.

Figure 6 shows the daily mean homogenised total ozone column record from 1990 to 2024, obtained by merging six collocated spectrophotometers. The uncertainty of the combined instruments is illustrated in the figure as error bars. The resulting TCO time series values ranged from 253 to 407 DU, for 95% coverage, with a median value of 312.93 DU for the 1990 to 2024 period.

https://doi.org/10.5194/egusphere-2026-6120
Preprint. Discussion started: 24 November 2026
© Author(s) 2026. CC BY 4.0 License.

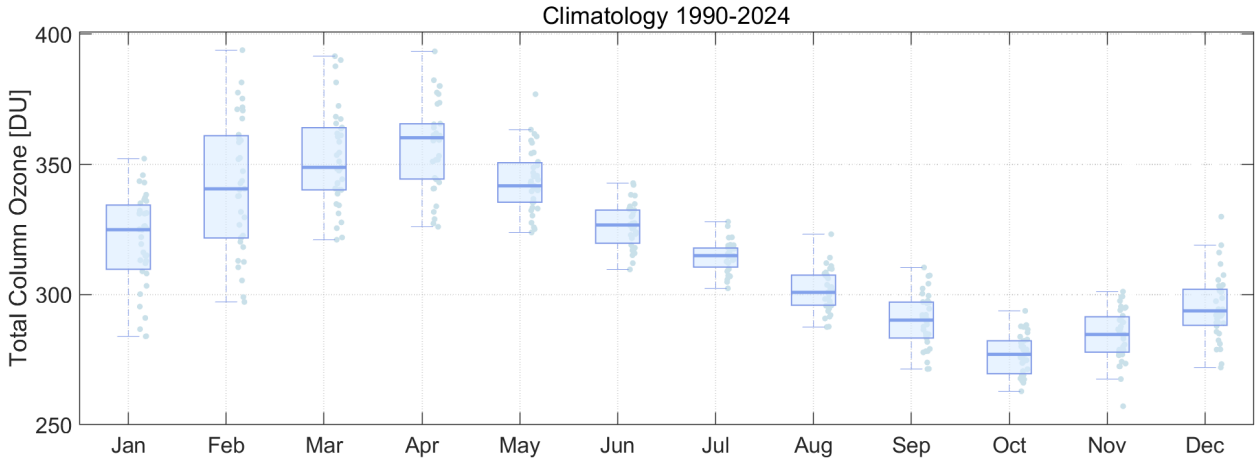

Figure 7. Monthly climatology of TCO at Arosa/Davos for the period 1990–2024. Each monthly boxplot is based on 35 monthly mean values. Boxes represent the interquartile range (25th–75th percentiles), the horizontal line indicates the median, whiskers extend to 1.5 times the interquartile range, and the dots show the individual monthly mean values. The dots are horizontally offset for visualization purposes only.

To further characterize the seasonal behaviour of the homogenised record, the monthly climatology was calculated over the 35-year period. Figure 7 shows the Arosa/Davos TCO climatology for the period 1990–2024. Each monthly climatological value is based on 35 monthly mean values, one from each year. The climatology exhibits a well-defined annual cycle, with maximum TCO values occurring in spring (March–April) and minimum values in autumn (October). The interannual variability, represented by the boxplots, is largest during late winter and spring, particularly in February and March, and generally decreases during summer and autumn.

To assess the consistency of the individual instruments contributing to the composite dataset, the relative differences of each instrument with respect to the composite product is shown in Figure 8, the top panel contains the relative differences of all six instruments, while the individual panels show the relative differences for each instrument respect to the composite. The figure demonstrates that all instruments are within $\pm 1\%$ except for B072; prior to the early 2000s, its relative differences were larger, reaching up to 2.5%, although the origin of this discrepancy remains unknown. The long-term agreement and stability among these multiple instruments over more than 20 years reflect the quality of instrument maintenance at the Arosa and Davos stations, and demonstrates the high quality of the Arosa/Davos TCO time series.

Figure 9 illustrates the impact of the harmonisation procedure by comparing the monthly median relative differences between the Dobson and Brewer measurements for the dataset using the Bass and Paur ozone cross sections and no effective ozone temperature correction (operational dataset), with the TCO derived using the Serdyuchenko ozone absorption cross sections and the effective ozone temperature correction (harmonised dataset), for the period from 2000 to 2014. The operational

https://doi.org/10.5194/egusphere-2026-6120
Preprint. Discussion started: 24 November 2026
© Author(s) 2026. CC BY 4.0 License.

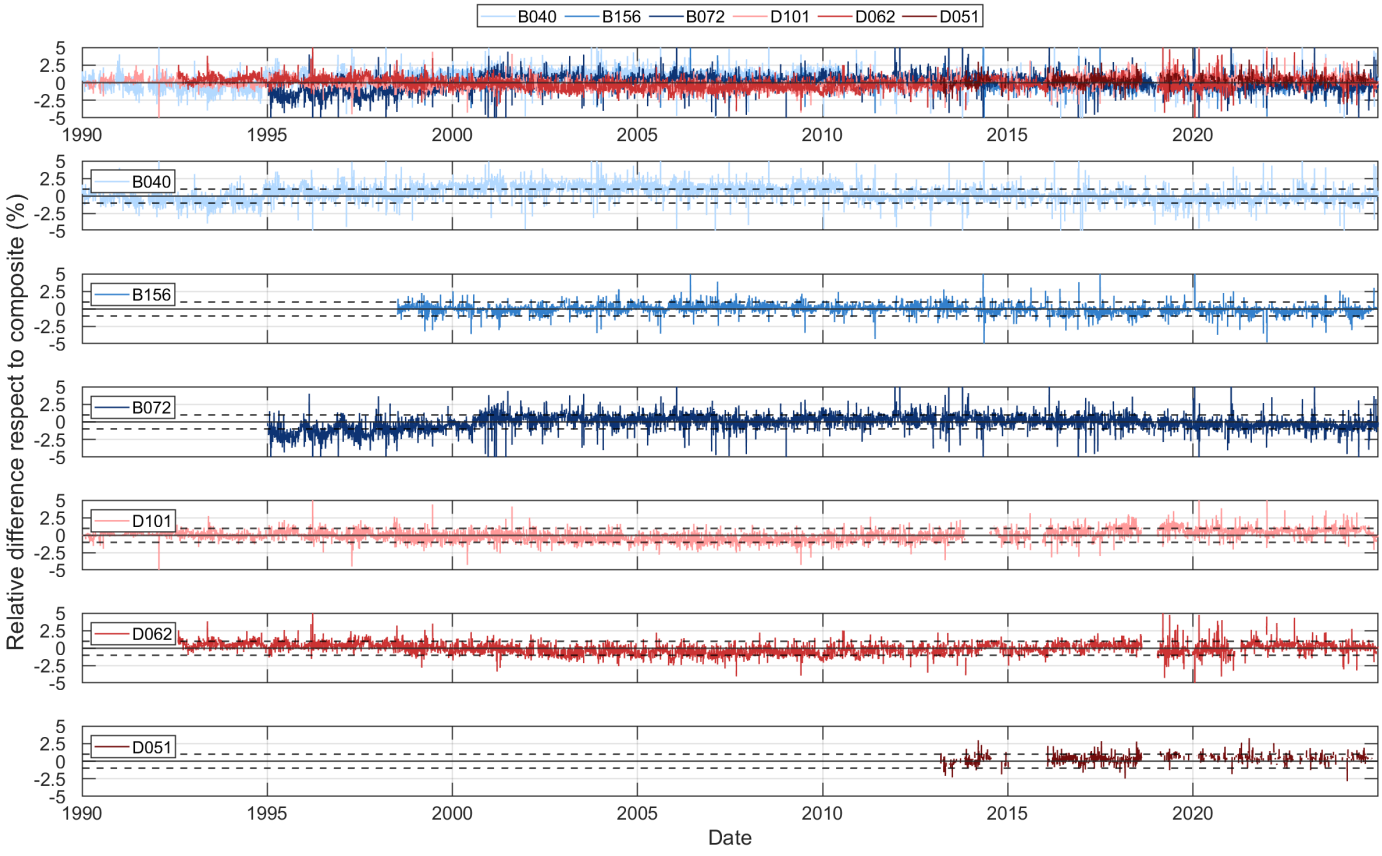

Figure 8. Relative TCO differences of all instruments relative to the merged composite (top panel). The relative TCO differences to the composite are shown in the lower panels for each instrument separately. The dashed lines indicate the $\pm 1\%$ relative difference. Blue colors correspond to the Brewer triad, and red colors the Dobson triad.

datasets relative differences shows a pronounced seasonal pattern, with larger differences in the winter season. In contrast, the harmonised datasets relative difference shows no seasonal cycle between the Dobson and Brewer TCO monthly mean values. These results confirm the findings from Redondas et al. (2014) and Gröbner et al. (2021) and demonstrate that the corrections proposed by Voglmeier et al. (2024) and adapted here are able to significantly improve the consistency between the TCO retrievals of Brewer and Dobson spectrophotometers.

The harmonised Dobson and Brewer TCO datasets differ by a relative offset of -0.7%. This difference is less than the combined uncertainty of $\pm 1.5\%$, estimated from the relative uncertainty of the two datasets using standard uncertainty propagation method.

https://doi.org/10.5194/egusphere-2026-6120
Preprint. Discussion started: 24 November 2026
© Author(s) 2026. CC BY 4.0 License.

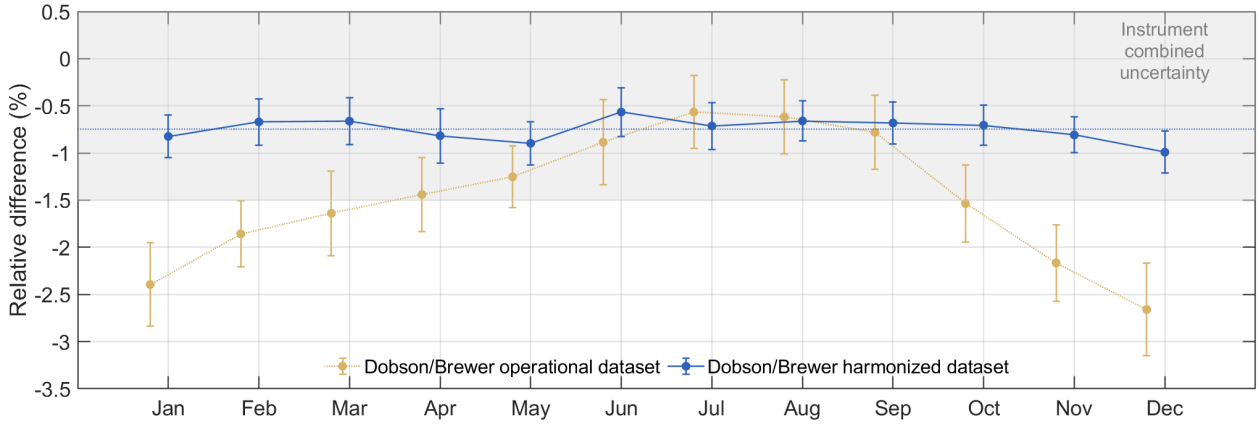

Figure 9. Relative differences between Dobson and Brewer monthly-median TCO over the period 2000-2014. The yellow and blue curves represent the operational and the harmonised datasets, respectively. The shaded area shows the combined uncertainty, while the blue dotted line represents the constant offset of the harmonised dataset.

4 Conclusions

The Arosa/Davos TCO time series is the world longest continuous TCO record. This study presents the TCO dataset and the procedures used to develop the homogenised TCO time series spanning the period from 1990 to 2024. This was achieved using six-co-located spectrophotometers: three Brewer and three automated Dobson instruments.

The most significant difference from previous studies was the implementation of the ozone absorption cross-sections from Serdyuchenko et al. (2014) for both Brewer and Dobson records and the application of the ozone effective temperature records based on ozone sonde data from Payerne, Switzerland. For the Brewer instruments, the TCO dataset was obtained using a method based on the standard lamp record of the instruments across their entire record, along with the calibration results from the RBCC-E campaigns. The Dobson TCO dataset was obtained in a similar way, using the calibrations from the Regional Dobson Calibration campaigns organised every 5 to 6 years.

A major strength of our study is the characterization of the uncertainty of each instrument based on its most relevant instrumental parameters. We find that, for smaller ozone slant columns, the uncertainties of the Brewer instruments are similar, and are mainly due to uncertainty in the instrument calibration factor, ETC. In contrast, at larger ozone slant columns, the relative uncertainties for single-monochromator Brewers increase significantly due to the impact of stray-light, whereas double-monochromator Brewers are less affected. Regarding Dobson uncertainties, they were formally evaluated using Monte-Carlo simulations that incorporate primary instrumental parameters, such as wavelength calibration uncertainty, wedge calibrations, slit functions, and lamp test variations. This yields a consistent overall uncertainty of $\sim 1\,\%$ across the automated Dobson triad for all ozone slant paths. The well-defined uncertainties of each TCO measurement from the individual instruments led to a composite merged dataset enhancing the reliability of the Arosa/Davos dataset, and providing a TCO time series with well

https://doi.org/10.5194/egusphere-2026-6120
Preprint. Discussion started: 24 November 2026
© Author(s) 2026. CC BY 4.0 License.

defined and reduced uncertainties on a daily scale. To ensure the homogeneity of the time series, we carefully re-evaluated the instrument relocation from Arosa to Davos during the 2011 to 2021 time period, and found that the relative TCO differences between Arosa and Davos (0.33± 0.78%) are consistent with the differences in the tropospheric ozone content between the two sites (0.28 ± 0.13%).

The Arosa/Davos TCO time series composite from six instruments, was produced using the Paule-Mandel technique. The composite consists in the weighted mean of the six instruments, with the weights computed from their respective uncertainties. Our homogenised time series presents a temporal coverage of $\sim 90\%$ days considering the period from the beginning of 1990 to the end of 2024 The daily uncertainty remains temporally-consistent across the record, with daily TCO values typically ranging from 1.0 (0.32%) to 3.4 (1.1%) DU (10th to 90th percentiles). The instruments are highly consistent with each other and deviate typically by less than 1% from the TCO composite, except for B072 during the initial 1995-2000 for reasons that are not yet understood.

Due to the high quality of the measurements, the robust characterization, and the use of six collocated instruments, this homogenised TCO record offers high reliability. Consequently, this time series serves as a promising benchmark dataset for detecting long-term ozone changes and the expected recovery of the ozone layer at mid-latitudes during this century. The scope of future research will be to detect the ozone recovery signal by comparing these observations with those from other stations across Europe and the Alps.

Data Availability. The dataset will be submitted to the World Ozone and Ultraviolet Radiation Data Centre (WOUDC) and will be made publicly available upon publication.

Author Contribution. FCH Analysed the dataset, produced the time series and wrote the manuscript. JG, supervised the research process, contributed to the discussion and interpretation of the analysis, and commented on the manuscript. LE responsible scientist of the quality control management of the instruments, and performed the Dobson uncertainty analysis and wrote that section on the manuscript. FZ is the instrument operator and performs the instrument maintenance. EMB and RR responsible scientists for the Arosa and Davos total column ozone time series and provide comments on the manuscript. GS supervised the research process and commented on the manuscript.

Competing Interests. The authors declare that they have no conflict of interest.

Acknowledgments. This research has been supported by the Swiss National Science Foundation **S**tratospheric and **T**ropospheric **O**zone over the **A**lps and Europe (STOA) project 200021L-228149. AI tools, such as ChatGPT, were used in this work to assist with sentence composition and language editing.

https://doi.org/10.5194/egusphere-2026-6120
Preprint. Discussion started: 24 November 2026
© Author(s) 2026. CC BY 4.0 License.

References

Ball, W. T., Alsing, J., Mortlock, D. J., Rozanov, E. V., Tummon, F., and Haigh, J. D.: Reconciling differences in stratospheric ozone composites, Atmos. Chem. Phys., **17**, 12269–12302, https://doi.org/10.5194/acp-17-12269-2017, 2017.

Bass, A. M. and Paur, R. J.: The ultraviolet cross-sections of ozone, I – The measurements, II – Results and temperature dependence, in: Atmospheric Ozone, edited by: Zerefos, C. S. and Ghazi, A., Springer, Dordrecht, The Netherlands, 606–616, https://doi.org/10.1007/978-94-009-5313-0_120, 1985.

Berjón, A., Redondas, A., Sildoja, M.-M., Nevas, S., Wilson, K., León-Luis, S. F., el Gawhary, O., and Fountoulakis, I.: Sensitivity study of the instrumental temperature corrections on Brewer total ozone column measurements, Atmos. Meas. Tech., **11**, 3323–3337, https://doi.org/10.5194/amt-11-3323-2018, 2018.

Bodeker, G. E., Nitzbon, J., Tradowsky, J. S., Kremser, S., Schwertheim, A., and Lewis, J.: A global total column ozone climate data record, Earth Syst. Sci. Data, **13**, 3885–3906, https://doi.org/10.5194/essd-13-3885-2021, 2021.

Bodhaine, B. A., Wood, N. B., Dutton, E. G., and Slusser, J. S.: On Rayleigh Optical Depth Calculations, J. Atmos. Ocean. Tech., 16, 1854–1861, 1999

Brewer, A.W. A replacement for the Dobson spectrophotometer?. PAGEOPH 106, 919–927 (1973). https://doi.org/10.1007/BF00881042

Brönnimann, S.: Century-long column ozone records show that chemical and dynamical influences counteract each other, Commun. Earth Environ., **3**, 143, https://doi.org/10.1038/s43247-022-00472-z, 2022.

Butchart, N.: The Brewer-Dobson circulation, Rev. Geophys., **52**, 157–184, https://doi.org/10.1002/2013RG000448, 2014.

Chipperfield, M. P. and Bekki, S.: Opinion: Stratospheric ozone – depletion, recovery and new challenges, Atmos. Chem. Phys., **24**, 2783–2802, https://doi.org/10.5194/acp-24-2783-2024, 2024.

Chipperfield, M., Bekki, S., Dhomse, S., and structures, A.: Detecting recovery of the stratospheric ozone layer, Nature, **549**, 211–218, https://doi.org/10.1038/nature23681, 2017.

Dobson, G. M. B., (1957) Observers' handbook for the ozone spectrophotometer, in Annals of the International Geophysical Year, V, Part 1, 46-89, Pergamon Press.

Egli, L., Gröbner, J., Hülsen, G., Schill, H., and Stübi, R.: Traceable total ozone column retrievals from direct solar spectral irradiance measurements in the ultraviolet, Atmos. Meas. Tech., **15**, 1917–1930, https://doi.org/10.5194/amt-15-1917-2022, 2022.

Egli, L., Gröbner, J., Schill, H., and Maillard Barras, E.: Total column ozone retrieval from a novel array spectroradiometer, Atmos. Meas. Tech., 16, 2889–2902, https://doi.org/10.5194/amt-16-2889-2023, 2023.

Egorova, T., Rozanov, E., Gröbner, J., Hauser, M., and Schmutz, W.: Montreal Protocol Benefits simulated with CCM SOCOL, Atmos. Chem. Phys., **13**, 3811–3823, https://doi.org/10.5194/acp-13-3811-2013, 2013.

Evans, R. D.: Operations Handbook–Ozone Observations with a Dobson Spectrophotometer, rev. ed., Rep. 183, Global Atmosphere Watch, World Meteorological Organization, Geneva, Switzerland, 2008. https://library.wmo.int/idurl/4/47538

Farman, J. C., Gardiner, B. G., and Shanklin, J. D.: Large losses of total ozone in Antarctica reveal seasonal ClOx/NOx interaction, Nature, **315**, 207–210, https://doi.org/10.1038/315207a0, 1985.

Fioletov, V. E., Bodeker, G. E., Miller, A. J., McPeters, R. D., and Stolarski, R.: Global and zonal total ozone variations estimated from ground-based and satellite measurements: 1964–2000, J. Geophys. Res., **107**, 4647, https://doi.org/10.1029/2001JD001350, 2002.

Götz, F. W. P., Meetham, A. R., and Dobson, G. M. B.: The vertical distribution of ozone in the atmosphere, P. R. Soc. Lond. A, **145**, 416–446, 1934.

https://doi.org/10.5194/egusphere-2026-6120
Preprint. Discussion started: 24 November 2026
© Author(s) 2026. CC BY 4.0 License.

Gröbner, J., Schill, H., Egli, L., and Stübi, R.: Consistency of total column ozone measurements between the Brewer and Dobson spectroradiometers of the LKO Arosa and PMOD/WRC Davos, Atmos. Meas. Tech., **14**, 3319–3331, https://doi.org/10.5194/amt-14-3319-2021, 2021.

Hassler, B., Petropavlovskikh, I., Staehelin, J., August, T., Bhartia, P. K., Clerbaux, C., Degenstein, D., Mazière, M. D., Dinelli, B. M., Dudhia, A., Dufour, G., Frith, S. M., Froidevaux, L., Godin-Beekmann, S., Granville, J., Harris, N. R. P., Hoppel, K., Hubert, D., Kasai, Y., Kurylo, M. J., Kyrölä, E., Lambert, J.-C., Levelt, P. F., McElroy, C. T., McPeters, R. D., Munro, R., Nakajima, H., Parrish, A., Raspollini, P., Remsberg, E. E., Rosenlof, K. H., Rozanov, A., Sano, T., Sasano, Y., Shiotani, M., Smit, H. G. J., Stiller, G., Tamminen, J., Tarasick, D. W., Urban, J., van der A, R. J., Veefkind, J. P., Vigouroux, C., von Clarmann, T., von Savigny, C., Walker, K. A., Weber, M., Wild, J., and Zawodny, J. M.: Past changes in the vertical distribution of ozone – Part 1: Measurement techniques, uncertainties and availability, Atmos. Meas. Tech., **7**, 1395–1427, https://doi.org/10.5194/amt-7-1395-2014, 2014.

Hegglin, M. I., Fahey, D. W., McFarland, M., Montzka, S. A., and Nash, E. R.: Twenty Questions and Answers About the Ozone Layer: 2014 Update, Scientific Assessment of Ozone Depletion: 2014, World Meteorological Organization, Geneva, Switzerland, 2015. Available at https://csl.noaa.gov/assessments/ozone/2014/twentyquestions2014update.pdf

Iglewicz, B. and Hoaglin, D. C.: How to Detect and Handle Outliers, ASQC Basic References in Quality Control, Vol. 16, ASQC Quality Press, Milwaukee, USA, ISBN 978-0-87389-247-6, 1993.

JCGM: Evaluation of measurement data – Guide to the expression of uncertainty in measurement, JCGM 100:2008, Joint Committee for Guides in Metrology, BIPM, Sèvres, France, available at: https://www.bipm.org/documents/20126/2071204/JCGM_100_2008_E.pdf, 2008.

Kerr, J. B., McElroy, C. T., and Olafson, R. A.: Measurements of Ozone with the Brewer Ozone Spectrophotometer, Proc. Inter. Ozone Symposium, Boulder, 74–79, 1980a.

Kerr, J. B., McElroy, C. T., Wardle, D. I., Olafson, R. A., and Evans, W. F. J.: The Automated Brewer Spectrophotometer, in: Atmospheric Ozone, edited by: Zerefos, C. S. and Ghazi, A., Springer, Dordrecht, https://doi.org/10.1007/978-94-009-5313-0_80, 1985.

Kerr, J. B., McElroy, C. T., and Evans, W. F. J.: The automated Brewer spectrophotometer for measurement of SO2, O3, and aerosols, Symposium on Meteorological Observations and Instrumentation, 470–472, World Meteorol. Organ./Am. Meteorol. Soc./CMOS, Toronto, Ontario, Canada, 1983.

Kerr, J. B., Asbridge, I. A., and Evans, W. F. J.: Intercomparison of total ozone measured by the Brewer and Dobson spectrophotometers at Toronto, J. Geophys. Res., 93(D9), 11129–11140, https://doi.org/10.1029/JD093iD09p11129, 1988.

Kerr, J. B.: New methodology for deriving total ozone and other atmospheric variables from Brewer spectrophotometer direct sun spectra, J. Geophys. Res., **107**, 4731, https://doi.org/10.1029/2001JD001227, 2002.

Köhler, U., Nevas, S., McConville, G., Evans, R., Smid, M., Stanek, M., Redondas, A., and Schönenborn, F.: Optical characterisation of three reference Dobsons in the ATMOZ Project verification of G. M. B. Dobson's original specifications, Atmos. Meas. Tech., **11**, 1989–1999, https://doi.org/10.5194/amt-11-1989-2018, 2018.

Komhyr, W. D.: Dobson spectrophotometer systematic total ozone measurement error, Geophys. Res. Lett., **7**, 161–163, https://doi.org/10.1029/GL007i002p00161, 1980.

Komhyr, W. D., Grass, R. D., and Leonard, R. K.: Dobson spectrophotometer 83: A standard for total ozone measurements, 1962–1987, J. Geophys. Res., 94(D7), 9847–9861, https://doi.org/10.1029/JD094iD07p09847, 1989.

https://doi.org/10.5194/egusphere-2026-6120
Preprint. Discussion started: 24 November 2026
© Author(s) 2026. CC BY 4.0 License.



Koukouli, M. E., Zara, M., Lerot, C., Fragkos, K., Balis, D., van Roozendael, M., Allart, M. A. F., and van der A, R. J.: The impact of the ozone effective temperature on satellite validation using the Dobson spectrophotometer network, Atmos. Meas. Tech., **9**, 2055–2065, https://doi.org/10.5194/amt-9-2055-2016, 2016.

Labow, G. J., McPeters, R. D., Bhartia, P. K., and Kramarova, N.: A comparison of 40 years of SBUV measurements of column ozone with data from the Dobson/Brewer network, J. Geophys. Res. Atmos., **118**, 7370–7378, https://doi.org/10.1002/jgrd.50503, 2013.

León-Luis, S. F., Redondas, A., Carreño, V., López-Solano, J., Berjón, A., Hernández-Cruz, B., and Santana-Díaz, D.: Internal consistency of the Regional Brewer Calibration Centre for Europe triad during the period 2005–2016, Atmos. Meas. Tech., **11**, 4059–4072, https://doi.org/10.5194/amt-11-4059-2018, 2018.

Maillard Barras, E., Haefele, A., Stübi, R., Jouberton, A., Schill, H., Petropavlovskikh, I., Miyagawa, K., Stanek, M., and Froidevaux, L.: Dynamical linear modeling estimates of long-term ozone trends from homogenized Dobson Umkehr profiles at Arosa/Davos, Switzerland, Atmos. Chem. Phys., **22**, 14283–14302, https://doi.org/10.5194/acp-22-14283-2022, 2022.

Newman, P. A., Oman, L. D., Douglass, A. R., Fleming, E. L., Frith, S. M., Hurwitz, M. M., Kawa, S. R., Jackman, C. H., Krotkov, N. A., Nash, E. R., Nielsen, J. E., Pawson, S., Stolarski, R. S., and Velders, G. J. M.: What would have happened to the ozone layer if chlorofluorocarbons (CFCs) had not been regulated?, Atmos. Chem. Phys., **9**, 2113–2128, https://doi.org/10.5194/acp-9-2113-2009, 2009.

NOAA: National Oceanic and Atmospheric Administration (NOAA), US Standard Atmosphere, NOAA-S/T 76-1562, 1976.

Orphal, J., Staehelin, J., Tamminen, J., Braathen, G., De Backer, M.-R., Bais, A., Balis, D., Barbe, A., Bhartia, P. K., Birk, M., Burkholder, J. B., Chance, K., von Clarmann, T., Cox, A., Degenstein, D., Evans, R., Flaud, J.-M., Flittner, D., Godin-Beekmann, S., Gorshelev, V., Gratien, A., Hare, E., Janssen, C., Kyrölä, E., McElroy, T., McPeters, R., Pastel, M., Petersen, M., Petropavlovskikh, I., Picquet-Varrault, B., Pitts, M., Labow, G., Rotger-Languereau, M., Leblanc, T., Lerot, C., Liu, X., Moussay, P., Redondas, A., Van Roozendael, M., Sander, S. P., Schneider, M., Serdyuchenko, A., Veefkind, P., Viallon, J., Viatte, C., Wagner, G., Weber, M., Wielgosz, R. I., and Zehner, C.: Absorption cross-sections of ozone in the ultraviolet and visible spectral regions: Status report 2015, J. Mol. Spectrosc., **327**, 105–121, https://doi.org/10.1016/j.jms.2016.07.007, 2016.

Paule, R. C. and Mandel, J.: Consensus Values and Weighting Factors, J. Res. Natl. Bur. Stand., **87**, 377–385, https://doi.org/10.6028/jres.087.022, 1982.

Paule, R. C. and Mandel, J.: Consensus Values, Regressions, and Weighting Factors, J. Res. Natl. Inst. Stand. Technol., **94**, 197–203, https://doi.org/10.6028/jres.094.020, 1989.

Petropavlovskikh, I., Bhartia, P. K., and DeLuisi, J.: New Umkehr ozone profile retrieval algorithm optimized for climatological studies, Geophys. Res. Lett., **32**, L16808, https://doi.org/10.1029/2005GL023323, 2005.

Redondas, A., Evans, R., Stuebi, R., Köhler, U., and Weber, M.: Evaluation of the use of five laboratory-determined ozone absorption cross sections in Brewer and Dobson retrieval algorithms, Atmos. Chem. Phys., **14**, 1635–1648, https://doi.org/10.5194/acp-14-1635-2014, 2014.

Redondas, A., Nevas, S., Berjón, A., Sildoja, M.-M., León-Luis, S. F., Carreño, V., and Santana-Díaz, D.: Wavelength calibration of Brewer spectrophotometer using a tunable pulsed laser and implications to the Brewer ozone retrieval, Atmos. Meas. Tech., **11**, 3759–3768, https://doi.org/10.5194/amt-11-3759-2018, 2018.

Redondas, A., Berjón, A., López-Solano, J., Carreño, V., León-Luis, S. F., and Santana-Díaz, D.: Fourteenth Intercomparison Campaign of the Regional Brewer Calibration Centre Europe, Joint publication of State Meteorological Agency (AEMET), Madrid, Spain and World Meteorological Organization (WMO), Geneva, Switzerland, WMO/GAW Report No. 257, https://library.wmo.int/records/item/57415-fourteenth-intercomparison-campaign-of-the-regional-brewer-calibration-centre-europe, 2021.

https://doi.org/10.5194/egusphere-2026-6120
Preprint. Discussion started: 24 November 2026
© Author(s) 2026. CC BY 4.0 License.

Redondas, A., Parra-Rojas, F., López-Solano, J., and Berjón, A.: Eubrewnet Uncertainty Budget-WP1: Total ozone uncertainty model on Brewer Algorithm due to instrumental parameters, Tech. rep., ESA, http://rbcce.aemet.es/dokuwiki/doku.php?id=codes:errorbudget, 2020.

Rozanov, E., Egorova, T., Egli, L., Karagodin-Doyennel, A., Sukhodolov, T., Schill, H., Stübi, R., and Gröbner, J.: Representativeness of the Arosa/Davos Measurements for the Analysis of the Global Total Column Ozone Behavior, Front. Earth Sci., **9**, 675084, https://doi.org/10.3389/feart.2021.675084, 2021.

Scarnato, B., Staehelin, J., Stübi, R., and Schill, H.: Long-term total ozone observations at Arosa (Switzerland) with Dobson and Brewer instruments (1988–2007), J. Geophys. Res., **115**, D13306, https://doi.org/10.1029/2009JD011908, 2010.

Scarnato, B., Staehelin, J., Peter, T., Groebner, J., and Stuebi, R.: Temperature and slant path effects in Dobson and Brewer total ozone measurements, J. Geophys. Res., 114, D24303, https://doi.org/10.1029/2009JD012349, 2009.

Serdyuchenko, A., Gorshelev, V., Weber, M., Chehade, W., and Burrows, J. P.: High spectral resolution ozone absorption cross-sections – Part 2: Temperature dependence, Atmos. Meas. Tech., **7**, 625–636, https://doi.org/10.5194/amt-7-625-2014, 2014.

Smid, M., Porrovecchio, G., Tesar, J., Burnitt, T., Egli, L., Gröbner, J., Linduska, P., and Stanek, M.: The design and development of a tuneable and portable radiation source for in situ spectrometer characterisation, Atmos. Meas. Tech., **14**, 3573–3582, https://doi.org/10.5194/amt-14-3573-2021, 2021.

Staehelin, J., Renaud, A., Bader, J., McPeters, R., Viatte, P., Hoegger, B., Bugnion, V., Giroud, M., and Schill, H.: Total ozone series at Arosa (Switzerland): Homogenization and data comparison, J. Geophys. Res., **103**, 5827–5841, https://doi.org/10.1029/97JD02402, 1998a.

Staehelin, J., Kegel, R., and Harris, N. R. P.: Trend analysis of the homogenized total ozone series of Arosa (Switzerland), 1926–1996, J. Geophys. Res., **103**, 8389–8399, https://doi.org/10.1029/97JD03650, 1998b.

Staehelin, J., Kerr, J., Evans, R., and Vanicek, K.: Comparison of Total Ozone Measurements of Dobson and Brewer Spectrophotometers and Recommended Transfer Functions, GAW Report No. 149 (WMO TD No. 1147), World Meteorological Organization, Geneva, 2003.

Staehelin, J., Viatte, P., Stübi, R., Tummon, F., and Peter, T.: Stratospheric ozone measurements at Arosa (Switzerland): history and scientific relevance, Atmos. Chem. Phys., **18**, 6567–6584, https://doi.org/10.5194/acp-18-6567-2018, 2018.

Stübi, R., Schill, H., Klausen, J., Maillard Barras, E., and Haefele, A.: A fully automated Dobson sun spectrophotometer for total column ozone and Umkehr measurements, Atmos. Meas. Tech., **14**, 5757–5769, https://doi.org/10.5194/amt-14-5757-2021, 2021.

Stübi, R., Schill, H., Klausen, J., Vuilleumier, L., Gröbner, J., Egli, L., and Ruffieux, D.: On the compatibility of Brewer total column ozone measurements in two adjacent valleys (Arosa and Davos) in the Swiss Alps, Atmos. Meas. Tech., **10**, 4479–4490, https://doi.org/10.5194/amt-10-4479-2017, 2017.

Stübi, R., Schill, H., Klausen, J., Vuilleumier, L., and Ruffieux, D. C.: Reproducibility of total ozone column monitoring by the Arosa Brewer spectrophotometer triad, J. Geophys. Res. Atmos., 122, 4735–4745, https://doi.org/10.1002/2016JD025735, 2017.

Steinbrecht, W., Hegglin, M. I., Harris, N., and Weber, M.: Is global ozone recovering?, Comptes Rendus Geoscience, 350(7), 368–375, https://doi.org/10.1016/j.crte.2018.07.012, 2018.

Vanicek, K.: Differences between ground Dobson, Brewer and satellite TOMS-8, GOME-WFDOAS total ozone observations at Hradec Kralove, Czech, Atmos. Chem. Phys., **6**, 5163–5171, https://doi.org/10.5194/acp-6-5163-2006, 2006.

Voglmeier, K., Velazco, V. A., Egli, L., Gröbner, J., Redondas, A., and Steinbrecht, W.: The transition to new ozone absorption cross sections for Dobson and Brewer total ozone measurements, Atmos. Meas. Tech., **17**, 2277–2294, https://doi.org/10.5194/amt-17-2277-2024, 2024.

WMO (World Meteorological Organization): Scientific Assessment of Ozone Depletion: 2022, GAW Report No. 278, 509 pp., WMO, Geneva, ISBN 978-9914-733-97-6, https://csl.noaa.gov/assessments/ozone/2022/ (last access: 16 November 2026), 2022.

https://doi.org/10.5194/egusphere-2026-6120
Preprint. Discussion started: 24 November 2026
© Author(s) 2026. CC BY 4.0 License.



Ziemke, J. R., Chandra, S., and Bhartia, P. K.:"Cloud slicing": A new technique to derive upper tropospheric ozone from satellite measurements, J. Geophys. Res., 106(D9), 9853–9867, https://doi.org/10.1029/2000JD900768, 2001.

685 Ziemke, J. R., Chandra, S., and Bhartia, P. K.: Upper tropospheric ozone derived from the cloud slicing technique: Implications for large-scale convection, J. Geophys. Res., 108(D13), 4390, https://doi.org/10.1029/2002JD002919, 2003.

Zuber, R., Köhler, U., Egli, L., Ribnitzky, M., Steinbrecht, W., and Gröbner, J.: Total ozone column intercomparison of Brewers, Dobsons, and BTS-Solar at Hohenpeißenberg and Davos in 2019/2020, Atmos. Meas. Tech., 14, 4915–4928, https://doi.org/10.5194/amt-14-4915-2021, 2021.